

# Kinetics and Thermodynamics of Type VIII $\beta$ -Turn Formation: A CD, NMR, and Microsecond Explicit Molecular Dynamics Study of the GDNP Tetrapeptide

Patrick F. J. Fuchs,\* Alexandre M. J. J. Bonvin,<sup>†</sup> Brigida Bochicchio,<sup>‡</sup> Antonietta Pepe,<sup>‡</sup> Alain J. P. Alix,<sup>§</sup> and Antonio M. Tamburro<sup>‡</sup>

\*Equipe de Bioinformatique Génomique et Moléculaire, INSERM U726, Université Paris 7, 75251 Paris Cedex 05, France;

<sup>†</sup>Bijvoet Center for Biomolecular Research, Utrecht University, 3584 CH Utrecht, The Netherlands; <sup>‡</sup>Dipartimento di Chimica,

Università degli Studi della Basilicata, 85100 Potenza, Italy; and <sup>§</sup>Laboratoire de Spectroscopies et Structures BioMoléculaires,

Université de Reims Champagne-Ardenne, Faculté des Sciences, BP 1039, 51687 Reims Cedex 2, France

**ABSTRACT** We report an experimental and theoretical study on type VIII  $\beta$ -turn using a designed peptide of sequence GDNP. CD and NMR studies reveal that this peptide exists in equilibrium between type VIII  $\beta$ -turn and extended conformations. Extensive MD simulations give a description of the free energy landscape of the peptide in which we retrieve the same two main conformations suggested by the experiments. The free energy difference between the two conformational states is very small and the transition between them occurs within a few kT at 300 K on a nanosecond timescale. The equilibrium is mainly driven by entropic contribution, which favors extended conformations over  $\beta$ -turns. This confirms other theoretical studies showing that  $\beta$ -turns are marginally stable in water solution because of the larger entropy of the extended state unless some stabilizing interactions exist. Our observations may be extended to any type of  $\beta$ -turn and have important consequences for protein folding. A comparison of our MD and CD results also suggests a possible type VIII  $\beta$ -turn CD signature indicated by one main band at 200 nm, close to that of random coil, and a fairly large shoulder at 220 nm. Last, our results clearly show that the XXXP motif can only fold into a type VIII  $\beta$ -turn, which is consistent with its fairly strong propensity for this type of turn. This important finding may help for peptide design and is in line with recent studies on bioactive elastin peptides.

## INTRODUCTION

$\beta$ -Turns represent an irregular type of secondary structure that allows the protein backbone to turn back on itself. They are considered as irregular because they are just defined by four residues ( $i$ ,  $i + 1$ ,  $i + 2$ ,  $i + 3$ ) whose properties do not show any periodicity like in the other classical secondary structure elements (i.e., the  $\phi / \psi$  or hydrogen bonding patterns in  $\alpha$ -helix or  $\beta$ -strand). They were first recognized by Venkatachalam (1) and later their definition was extended by Lewis et al. to any tetrapeptide whose  $C^\alpha_i - C^\alpha_{i+3}$  distance was shorter than 7 Å with the two central residues ( $i + 1$  and  $i + 2$ ) nonhelical (2). A few years later, Richardson introduced types VI  $\beta$ -turn with a *cis*-Pro at position  $i + 2$ , and proposed to reclassify the types introduced by Lewis et al. (3). She also noticed that some distorted type I  $\beta$ -turns could occur with the  $\phi / \psi$  of residue  $i + 1$  in the  $\alpha$ -region of the Ramachandran plot, and the  $i + 2$  in the  $\beta$ -region; she proposed to classify these latter as type Ib. Later, Wilmot and Thornton (4) refined the definition of type Ib and proposed to introduce a new type, that is type VIII, with precise values of

$\phi / \psi$  dihedral angles:  $-60^\circ$  and  $-30^\circ$  for residue  $i + 1$  and  $-120^\circ$  and  $120^\circ$  for residue  $i + 2$ . Actually, the accepted nomenclature uses the one of Hutchinson and Thornton (i.e., types I, I', II, II', VIII, VIa, VIb, and IV) (5).

$\beta$ -turns play many biological roles in peptides (6) and proteins (6,7). They are in most cases constituted by hydrophilic residues (5,8) and thus often occur at protein surface (5). This and the predominance of functional side chains (e.g., Asp, Ser, Pro, Thr, Lys) (5) give them a role as recognition site in proteins (e.g., in antibodies, enzymes, receptors, etc.) (6). Furthermore,  $\beta$ -turns confer some flexibility to proteins, which is important for many biochemical processes (9–12) and has implications in drug discovery (13), ligand binding (14), and protein-protein docking studies (15,16). Their intrinsic ease of formation and disruption and ability to “slide” from one tetrapeptide to its neighbor (18,19) might also play a role in the resilience of tropoelastin (17). In peptides,  $\beta$ -turns often play the role of bioactive conformation (6) (e.g., in hormones, degraded peptides involved in regulations, etc.) as shown recently for example in some elastin peptides (8,20,21), or in the complement inhibitor compstatin (22), etc. The relevance of  $\beta$ -turns for biological functions has led to a great deal of interest for mimicking their presence in the field of pharmacology (23,24).

$\beta$ -Turns also play a critical role in the three-dimensional architecture of proteins by orienting secondary structure elements such as  $\alpha$ -helices and/or  $\beta$ -strands. Moreover, it has been shown that they are involved in the folding of

Submitted September 12, 2005, and accepted for publication January 12, 2006.

Address reprint requests to Alexandre M. J. J. Bonvin, E-mail: a.m.j.j.bonvin@chem.uu.nl; or Antonio M. Tamburro, E-mail: tamburro@unibas.it.

**Abbreviations used:** CD, circular dichroism; NMR, nuclear magnetic resonance; MD, molecular dynamics; TFE, trifluoroethanol; SA, simulated annealing; SD, steepest descent; ABNR, adopted basis Newton-Raphson; RMS, root mean square; PDB, Protein Data Bank.

© 2006 by the Biophysical Society

0006-3495/06/04/2745/15 \$2.00

doi: 10.1529/biophysj.105.074401

$\beta$ -hairpins (25–30). In one of the mechanisms the  $\beta$ -turn is thought to form first (30), then the hydrogen bonds propagate along the strands. This mechanism is called “zip-up” and has been observed experimentally (28,29), as well as in MD simulations (31–33). Other mechanisms have been reported as well (34–36). In proteins,  $\beta$ -turns can affect the folding kinetics and the stability (37–39) (see Searle and Ciani (40) for a review). The nucleation of  $\beta$ -hairpin is thought to be an early step in protein folding (40), which shows the importance of  $\beta$ -turns within this context. Gu et al. (37), however, suggested that the role of  $\beta$ -turns in protein folding might be context dependent and therefore difficult to generalize.

$\beta$ -Turns formation, folding, and stability have been widely studied by computational methods since the beginning of the 1990s by means of peptide simulation studies (41–51). The main results indicate that  $\beta$ -turns fold in the nanosecond time range (45,47) and are marginally stable in water solution (42,48) unless some stabilizing features are present such as side-chain stacking (43), electrostatic interactions (49), hydrophobic packing (45), aromatic-amine interaction (50), hydrogen bonding (46), or charged-charged interactions (51). In parallel, a very large number of computational studies have been devoted to the determination of free energy differences of  $\beta$ -turn formation or interconversion using various sampling techniques (48,52–59). In some cases (33,60), kinetic aspects have also been considered. All the reported free energies of folding depend strongly on the sequence and type of turn and fall generally within a few kT (at 300 K); they usually do not exceed 25 or 30 kJ mol<sup>-1</sup> unless some steric incompatibilities are present. This means that  $\beta$ -turns are very easy to form and break; they exist always in equilibrium with some other conformations, generally extended ones (61). This capacity might be very important for protein folding.

Among the extremely large number of theoretical papers involving  $\beta$ -turns, most of them are focused on the hydrogen bonded classic types (I, II, I', II') and to a lesser extent on type VI (33,41–43,45–51,53–60). In contrast, there has been a little interest for type VIII despite the fact it occurs in proteins almost as much as type II (~9% of all  $\beta$ -turns) (5,8) and has been proposed to be the most important type in peptides (56). Once precisely defined (4), type VIII has been observed at the hinge of orthogonal  $\beta$ - $\beta$  motifs (62) and in MD simulations (21,63–65). It has been proposed to occur in an oxidized Cysteinil-Cysteine unit within the nicotinic acetylcholine receptor (66,67), and more generally within vicinal disulfide turns (68). Recently, Santa et al. calculated the free energy of formation of type VIII from a fully extended conformation (56): they found (for the sequence SALN as well as other mutants of the third amino acid) that type VIII presents a lower free energy than extended conformations. Based on those results, they proposed that type VIII could be the most important type of turn in peptides. Except for those few studies, type VIII has been poorly characterized, especially from the experimental point of view.

These last years, there has been a great deal of interest in the computational community to study peptide (and small protein) folding as this represents the early stage of protein folding (53). Daura et al. (69) suggested that deciphering the folding pathways of single peptides may not give general rules, but that analyzing a relevant number of examples may provide insights into this complex problem. They also emphasized the need to characterize both folded and unfolded states of peptides and the importance of understanding their dynamic behavior as suggested before (70). The explosion of computing capacity enabled us to simulate folding of peptides or small proteins in explicit solvent (71). Daura et al. (70,72,73) were able to fold and unfold a  $\beta$ -heptapeptide in methanol, Chipot et al. to fold some helical peptides at a water/hexane interface (74,75). In 1998, Duan and Kollman brought a milestone in explicit simulations by describing an early folding event of a small protein (the villin headpiece) in a microsecond molecular dynamics (76). Since then, distributed computing within the Folding@Home Project has offered opportunities that even supercomputer could not reach (77).

In this context, the lack of knowledge on type VIII turns encouraged us to work on this particular type using the GDNP tetrapeptide as representative. We characterized the peptide conformation by CD and NMR and assessed its dynamic behavior by 200-ns MD simulations at different temperatures that allowed us to obtain a complete picture of the kinetics and thermodynamics of type VIII folding. Our work should help in the interpretation of CD spectra of small peptides containing type VIII  $\beta$ -turn, shed light on the influence of the GDNP sequence in peptides and proteins, and give an additional example of peptide folding.

One additional reason to characterize type VIII  $\beta$ -turn is linked to the activity of some elastin derived peptides: previous work (20,78) has shown that some elastin peptides, containing the GXXPG motif, are able to upregulate the production of MMP-1 (matrix metallo-proteinase 1) on human skin fibroblasts. It has been postulated that the bioactive conformation could be a  $\beta$ -turn of type VIII showing the sequence GXXP. This hypothesis has been validated in some recent work showing that when type VIII  $\beta$ -turn was unable to be formed, no biological activity was observed (21,64). This important finding may be relevant as there are many GXXP motifs in tropoelastin (>100) (64).

## MATERIALS AND METHODS

### Sequence design

We chose a four-residue peptide because this corresponds to the length of a  $\beta$ -turn. A longer sequence would dilute the CD signal of pure type VIII (each new peptidic bond does so). Furthermore, to be coherent with our previous study on elastin peptides, we kept the bioactive motif GXXP. Analysis of the residue preferences for type VIII  $\beta$ -turn (8) indicates that this sequence is a good choice because Pro at position  $i + 3$  has a very large propensity ( $P = 4.55$ ) for this type, whereas it is almost equal to 0 for the

other types. For Gly in position  $i$ , the  $\beta$ -turn is slightly favored ( $P = 1.44$ ). For the two central residues, we chose those presenting the largest propensity (except proline that would have been problematic to study by NMR because of the lack of amide proton): Asp for position  $i + 1$  ( $P = 1.72$ ) and Asn for position  $i + 2$  ( $P = 1.94$ ). Moreover, the ability of these residues to form H-bonds between their side chain and the backbone is a feature that stabilizes the turn. A quick search of the PDB revealed that all GDNP sequences within proteins are found either in type VIII (or close to type VIII) or in extended conformations.

## Synthesis and purification of GDNP

The peptide was synthesized by solid-phase synthesis on an automatic synthesizer (model 431A of Applied Biosystems, Foster City, CA) using Fmoc/DCC/HOBt chemistry. Fmoc amino acids were purchased from Novabiochem (Laufelfingen, Switzerland) and form Inbios (Pozzouli, Italy). The peptides were detached from the resin support using 95% trifluoroacetic acid, dried and purified by high pressure liquid chromatography on a semipreparative C18 reverse-phase column. The purity was assessed by MALDI mass spectrometry. The peptide was synthesized with a C-terminal amide function with a rink amide resin to avoid diketopiperazine formation (because of the C-terminal Pro).

## Circular dichroism

CD spectra were recorded in a cylindrical cell of pathlength 0.1 cm on a Jasco J-600 dichrograph. The sample concentrations were adjusted to 0.1 mg/ml. The data are expressed in terms of the molar ellipticity  $[\theta]$  in units of  $\text{deg cm}^2 \text{ dmol}^{-1}$ .

## Nuclear magnetic resonance

All NMR experiments were performed on a Varian (Palo Alto, CA) Unity Inova 500 MHz spectrometer, equipped with a triple resonance (H, C, N)  $z$  axis PFG 5-mm solution probe head. Two-dimensional TOCSY and NOESY were acquired in the phase sensitive mode using States-Habercom technique with presaturation (2 s) of the water signal. The data were collected as 256 (t1) and 2048 (t2) complex point time domain matrix with a spectral width of 6000 Hz. The data were zero filled and Fourier transformed to give a  $2 \times 2$  K matrix after apodization with  $90^\circ$  shifted sine bell squared function. Classical procedures were employed for sequential resonance assignment. TOCSY spectra were used to identify spin systems of the amino acids, while NOESY spectra were used to obtain interresidue connectivities. All chemical shifts and J coupling constants are available as Supplementary Material.

## Conformational space exploration

To explore the conformational space accessible to GDNP, we used the CHARMM program (79) with the all atom CHARMM22 force field (80) and an implicit representation of the solvent by setting the dielectric constant to 80. The starting extended conformation was energy minimized until convergence (RMS energy gradient  $< 4.187 \cdot 10^{-4} \text{ kJ mol}^{-1} \text{ \AA}^{-1}$  ( $10^{-4} \text{ kcal mol}^{-1} \text{ \AA}^{-1}$ )) using a combination of steepest descent and adopted-basis Newton-Raphson (ABNR) algorithms. Random backbone dihedral angles were then taken to generate a new conformation that was minimized following the same protocol. Its energy was compared to the previous one: if lower, the new conformation was kept as the new reference, otherwise it was rejected. This procedure was repeated 100,000 times. This simple algorithm easily overcomes energy barriers. A plot of the dihedrals angles against each other indicated full coverage of conformational space.

## Molecular dynamics simulations

The MD simulations starting from a fully extended conformation were performed with GROMACS (81,82), using the GROMOS96 43A1 force

field (83). They were run in explicit water using the single point charge model (84), for 200 ns and at various temperatures. Analysis of the trajectories was performed using the programs included in the GROMACS package as well as some in house scripts.

The peptides were solvated in a cubic box of explicit water. The size of the box (38.8  $\text{\AA}$ ) was taken as the length of the peptide plus two times the nonbonded cutoff. The system comprised 2384 SPC molecules corresponding to a total number of 7189 atoms. The system was first energy minimized followed by equilibration with five successive 20-ps MD phases during which the force constant of the position restraints for the peptide was decreased from 1000 to 0  $\text{kJ mol}^{-1} \text{ nm}^{-2}$  (1000; 1000; 100; 10; 0). The initial velocities were generated at the desired temperatures following a Maxwellian distribution. All simulations were performed in the NPT ensemble by weakly coupling the system to external temperature and pressure baths (86), except for the first 20-ps equilibration part that was performed at constant volume (NVT).

A 2-fs time step was used for integrating the equations of motion using the leap frog algorithm. All bonds were constrained with the LINCS algorithm (87) and the water molecules were kept rigid using the SETTLE algorithm (88). Peptide and solvent were coupled separately to reference temperature baths with a time constant of 0.1 ps. The pressure was coupled to an external bath at 1 bar with a time constant of 0.5 ps and a compressibility of  $4.5 \times 10^{-5} \text{ bar}^{-1}$ . Periodic boundary conditions were applied all along the simulations. A twin-range cutoff of 0.8 and 1.4 nm was used for the nonbonded interactions in combination with a generalized reaction field correction beyond the 1.4-nm cutoff (89) using a dielectric constant of 54.

All simulations were performed in parallel on a LINUX cluster (1.3 and 2.6 GHz processors) and on 16 SGI ORIGIN 3000 CPUs (500 Mhz) at the Dutch national supercomputer center SARA in Amsterdam using the parallel version of GROMACS. As CPU cost indication, 1 ns took  $\sim 3$  h on both systems.

## RESULTS

### CD spectra of GDNP in water and in TFE

The CD spectra of GDNP in water and in TFE are reported in Fig. 1. Their shape is somewhat close to that of unordered conformations (90), with a major band centered around 200 nm corresponding to the  $\pi$ - $\pi^*$  transition, as well as a big shoulder at 220 nm corresponding to the  $n$ - $\pi^*$  transition. Usually, the band at 200 nm is assigned to the so-called random coil. The spectra show, however, some features that indicate that other conformations must exist. In fact, the spectra in TFE are higher in intensity as well; in literature, it has been shown many times that TFE favors  $\beta$ -turn conformations in small peptides (18,91) and more particularly in the case of type II  $\beta$ -turn (92–94). If we generalize this rule to any type of turn (because turns represent folded conformations) we must expect a higher CD signal in TFE than in water. In fact, the ellipticity in TFE is three times higher than that in water. Given the small size of the peptide and its high propensity for type VIII, we can assume that GDNP exists in a type VIII  $\beta$ -turn in solution in equilibrium with disordered (extended) conformations.

With respect to the temperature dependence, while only a very slight, if any, effect can be seen in TFE, a significant increase of the large negative band is noted in water when the temperature is decreased to  $0^\circ\text{C}$ . This could indicate the presence of both PPII conformation and  $\beta$ -turns that become

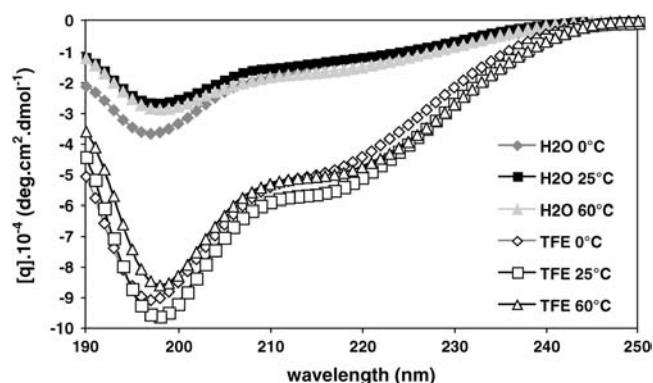


FIGURE 1 CD spectra of GDNP at different temperatures in water and in TFE.

avored at low temperature (95). Nevertheless, the absence of any isodichroic points clearly indicates the presence in both solutions of a complex mixture of conformations.

### NMR studies of GDNP

To validate our hypothesis, we studied GDNP by NMR in H<sub>2</sub>O(90%)/D<sub>2</sub>O(10%) at 278 and 298 K (the chemical shifts, the TOCSY and NOESY spectra, and the NOEs list are available as additional data). The analysis was performed on the 298 K data. Two subsets of signals are evident indicating that *cis/trans* isomerization occurs for the Pro-4 amide bond. The main isomer (90%) is *trans* and the following NMR data all refer to this predominant isomer. The occurrence of a strong  $d_{\text{aN}}$  ( $i, i + 1$ ) NOE crosspeak of residue Gly-1 and Asp-2, together with the absence of  $d_{\text{NN}}$  ( $i, i + 1$ ) NOE connectivity of residue Asp-2 and Asn-3 suggest the presence of extended conformations. The  $d_{\text{aN}}$  ( $i, i + 1$ ) NOE crosspeak for Asp-2–Asn-3 could not be identified at 298 K because of overlap with the water signal. The  $^3J_{\text{NH-H}\alpha}$  coupling constants are in the range 7–8 Hz (Asp-2 7.2 Hz; Asn-3 7.3 Hz), which can be due to conformational averaging as well as to a predominance of PPII conformation. At 278 K, the  $d_{\text{NN}}$  ( $i, i + 1$ ) NOE connectivity between residue Asp-2 and Asn-3 is still not detected, while it was possible to identify the  $d_{\text{aN}}$  ( $i, i + 1$ ) NOE crosspeaks between both Gly-1/Asp-2 and Asp-2/Asn-3 residues. Further, only the  $^3J_{\text{NH-H}\alpha}$  coupling constant of Asp-2 decreases from 7.2 to 7.0 Hz at 278 K, suggesting that the main conformational changes can be attributed to this residue. This J-coupling decrease at lower temperature indicates a slight change of Asp-2 toward the  $\alpha$ -region, which means more type VIII. This is thus consistent with the CD data in water that suggest more folded conformations at low temperatures.

NOE effects,  $^3J_{\text{NH-H}\alpha}$  coupling constants and H $\alpha$  chemical shifts reporting on the presence of type VIII  $\beta$ -turn are listed in Table 1 (all NMR data are provided as Supplementary Material). Two conditions have to be met to indicate the

presence of a type VIII  $\beta$ -turn for the GDNP sequence. First the proline at position 4 should be in a *trans* conformation. This can be monitored by the strong NOE between the  $\alpha$ -proton of Asn-3 and the  $\delta$ -protons of Pro-4, indicative of a short distance typical for a *trans* Pro (96). This is indeed the case for GDNP (see Table 1). Second, the distance between the amide proton of residue  $i + 1$ , Asp-2 in our case, and  $i + 2$ , Asn-3, should be short ( $< 3 \text{ \AA}$ ) indicating proper  $\phi/\psi$  dihedral angles ( $\phi = -60^\circ / \psi = -30^\circ$ ) as described by Wüthrich (96) for type I (which has the same  $\phi/\psi$  combination for residue  $i + 1$  as type VIII). This NOE could not be detected experimentally, although it should theoretically exist at least as a weak one because two consecutive amide protons cannot be  $> 5 \text{ \AA}$  apart. This could be explained by dynamical effects due to the conformational averaging in solution; its absence therefore does not preclude the existence of some population of type VIII in equilibrium with extended ones. Note also that solubility in water is an issue for this particular peptide sequence, which makes it difficult to detect weak NOEs.

Comparison of the experimental H $\alpha$  chemical shifts with those found in regular secondary structure of proteins (97) (see Table 1) adds an argument to the presence of an equilibrium between extended and turn conformations. The Asn-3-H $\alpha$  chemical shift is very close to that found in  $\beta$ -structures in proteins. This can be attributed to the presence of a proline at position 4, an amino acid known to force its preceding residue in the  $\beta$ -region (98,99). For Asp-2, the H $\alpha$  chemical shift is in between typical  $\alpha$ - and  $\beta$ -conformation, which suggests an equilibrium between the two. This is consistent with an equilibrium between extended (Asp-2 in the  $\beta$ -region) and type VIII (Asp-2 in the  $\alpha$ -region) conformations (see “Molecular dynamics” section below).

### Conformational space exploration

Because of the small size of GDNP it was possible to perform a full exploration of its energy surface. The complete  $\phi/\psi$  conformational space was explored by 100,000 steps of random drawing of dihedral angle values followed by energy minimization. The resulting lowest energy conformations are listed in Table 2. Two main energy wells are identified corresponding to extended (with a distance  $C_i^\alpha - C_{i+3}^\alpha$  almost equal to  $10 \text{ \AA}$ ) and “turn-like” conformations (with a  $C_i^\alpha - C_{i+3}^\alpha$  distance around  $7 \text{ \AA}$ ). The “turn-like” conformations are close to an ideal type VIII  $\beta$ -turn, with some minor deviations ( $< 45^\circ$ ) from the canonical dihedral angles values for this type of turn. The two lowest energy conformations (i.e., 46,303 and 70,764 in Table 2) can be considered as global minima for GDNP (under these particular conditions, i.e., in vacuum with the CHARMM22 all-atom force field using a dielectric constant of 80). They are very close in energy,  $1.3 \text{ kJ mol}^{-1}$ , within kT at 300 K, but correspond to two completely different conformations. Considering this small energy difference, their order (i.e., which one is the lowest

**TABLE 1** Comparison of relevant NMR experimental data with calculated ones: J-couplings, NOE effects, and  $^1\text{H}\alpha$  chemical shifts

	$J_{\text{Asp2}}$ (Hz)	$J_{\text{Asn3}}$ (Hz)			
Experimental values	7.25	7.35			
MD values					
All conformations	7.2 ( $\pm 2.4$ )	8.1 ( $\pm 2.2$ )			
Only type VIII conformations*	5.1 ( $\pm 2.2$ )	9.6 ( $\pm 0.5$ )			
Only extended conformations <sup>†</sup>	8.0 ( $\pm 2.1$ )	9.4 ( $\pm 0.9$ )			
Only PPII conformations <sup>‡</sup>	8.9 ( $\pm 1.5$ )	5.5 ( $\pm 1.1$ )			
	NOE $\text{NH}_{\text{Asp2}}\text{-NH}_{\text{Asn3}}$	NOE $\text{H}\alpha_{\text{Asn3}}\text{-H}\delta 1_{\text{Pro4}}$	NOE $\text{H}\alpha_{\text{Asn3}}\text{-H}\delta 1_{\text{Pro4}}$		
Experimental values	Not detected	Weak**	Weak**		
MD values (nm) <sup>§</sup>					
All conformations	0.34 $\pm$ 0.06	0.21 $\pm$ 0.03	0.21 $\pm$ 0.03		
Only type VIII conformations*	0.27 $\pm$ 0.04	0.21 $\pm$ 0.03	0.22 $\pm$ 0.03		
Only extended conformations <sup>†</sup>	0.43 $\pm$ 0.02	0.21 $\pm$ 0.03	0.21 $\pm$ 0.03		
Only PPII conformations <sup>‡</sup>	0.38 $\pm$ 0.04	0.22 $\pm$ 0.03	0.21 $\pm$ 0.03		
	Chemical shifts (ppm)				
	Experimental	Alpha <sup>¶</sup>	Beta <sup>¶</sup>	Coil <sup>¶</sup>	MD values <sup>  </sup>
H $\alpha$ Asp-2	4.77	4.43	4.94	4.60	4.6 ( $\pm 0.3$ )
H $\alpha$ Asn-3	5.00	4.48	5.06	4.66	4.8 ( $\pm 0.2$ )

Only the NOEs corresponding to distances that have to be short ( $< 0.3$  nm) to unambiguously define type VIII  $\beta$ -turn are presented.

\*Conformations with  $\text{C}_{\text{Gly1}}^{\alpha}\text{-C}_{\text{Pro4}}^{\alpha} < 0.7$  nm and  $\phi_{\text{Asn3}} < -100^{\circ}$ .

<sup>†</sup>Conformations with  $\text{C}_{\text{Gly1}}^{\alpha}\text{-C}_{\text{Pro4}}^{\alpha} > 1.0$  nm and  $\phi_{\text{Asn3}} < -100^{\circ}$ .

<sup>‡</sup>Conformations with  $\text{C}_{\text{Gly1}}^{\alpha}\text{-C}_{\text{Pro4}}^{\alpha} > 1.0$  nm and  $\phi_{\text{Asn3}} > -80^{\circ}$ .

<sup>§</sup>Calculated with the formula:  $r_{\text{ens}} = (\langle r^{-6} \rangle)^{-1/6}$  where  $r$  is the measured distance during the MD trajectory and  $r_{\text{ens}}$  the ensemble-averaged distance.

<sup>¶</sup>Reference values taken from Zhang et al. (97).

<sup>||</sup>Values calculated with the SHIFTCALC program (106).

\*\*These two NOEs were measured as weak ones experimentally, but the ratio of peaks volume between *cis* and *trans* isomer indicated 90% of *trans*, so these NOEs should be strong. One possible explanation might come from a problem of processing during the procedure of water suppression (because H $\alpha$  is close to the signal of water).

in energy) can easily vary under different conditions. This is indeed the case if another force field is used: with the GROMOS96 force field, type VIII becomes higher in energy than the extended conformation with a difference of  $2.9 \text{ kJ mol}^{-1}$ . This emphasizes the idea that not enthalpic but entropic effects must be the driving force that define the relative population of these two conformations in solution, as can be seen from our MD results (see next section).

## Molecular dynamics

To complement the experimental studies we performed various MD simulations of the GDNP tetrapeptide in explicit solvent using the GROMOS96 force field that has been shown previously to perform well for peptides (72,73). To get insight into the thermodynamics and kinetics of type VIII  $\beta$ -turn formation, 200-ns simulations were carried out in water at different temperatures (280, 300, 320, 340, and 360 K). Each trajectory was generated using different initial conditions to explore more conformational space. All simulations were run for *trans*-proline conformation because this was the major species in solution as indicated by the NMR data.

## Description of the MD trajectory at 300 K

In Fig. 2, we present the time evolution of some relevant observables (only the first 20 ns are shown for clarity): the

$\text{C}_{\text{Gly1}}^{\alpha}\text{-C}_{\text{Pro4}}^{\alpha}$  distance, which defines the presence (or absence) of turn conformations, and the  $\phi / \psi$  dihedral angle values of the two central residues  $i + 1$  and  $i + 2$ , which define the type of the turn. Many transitions between turn and extended conformations take place (this is also true at other temperatures) indicating that the free energy barrier must be within a few kT. Extended conformations occur more often than type VIII or type VIII-like conformations. A few conformations with positive  $\phi$ -values are observed, even in the  $\varepsilon$ -area of the Ramachandran map (positive  $\phi$  and negative  $\psi$ ), which is usually populated by glycines. Some of these conformations could correspond to a turn with positive  $\phi_{\text{Asp2}}$  and  $\psi_{\text{Asp2}}$  and Asn-3 in the  $\alpha$ -region; such a conformation is, however, unfavorable and is almost never met along the trajectory, surely because of steric hindrances.

Asn-3 is blocked in the  $\beta$ -conformation, with very rare visits to positive  $\phi$ -values;  $\psi$  is spectacularly blocked at a value around  $-120^{\circ} (\pm 20)$ . This is the main reason why Asn-3 lies in the  $\beta$ -area; this behavior comes from the effect of Pro-4 as observed previously (98,99). As a consequence, Pro-4 strongly favors type VIII formation because it forces the  $i + 2$  residue in the right conformation (5) and prevents the formation of any other type of  $\beta$ -turn because only type VIII possesses the  $i + 2$  residue in the  $\beta$ -conformation. The main degree of freedom in the GDNP tetrapeptide is thus  $\psi$  of Asp-2 as is clear from Fig. 2: it determines the peptide

**TABLE 2 Energetics and geometrical features of the lowest energy conformations of the conformational space search**

No.*	Energy (kJ mol <sup>-1</sup> )	$d_{C\alpha-C\alpha}$ (Å)	Type	$\Delta\phi_{i+1}$ (°)	$\Delta\psi_{i+1}$ (°)	$\Delta\phi_{i+2}$ (°)	$\Delta\psi_{i+2}$ (°)
00000	98.55	9.4	No turn	–	–	–	–
00005	98.23	9.3	No turn	–	–	–	–
00006	97.42	6.4	Type IV	27.2	43.6	32.7	20.7
00008	95.02	6.0	Type IV	23.6	35.7	32.3	20
00035	95.02	5.9	Type IV	23.7	35.7	32.4	20
00053	94.46	9.5	No turn	–	–	–	–
00080	91.17	6.3	Type IV	27	44	32.1	9.5
00169	90.84	6.1	Type IV	23.3	35.5	32.2	20.3
00495	90.18	6.7	Type IV	26.8	41.4	30.4	32.2
00856	88.17	6.5	Type IV	24.3	37.9	29.3	32.4
01581	88.17	6.5	Type IV	24.2	37.9	29.3	32.4
01910	88.17	6.4	Type IV	24.2	37.9	29.3	32.4
04662	87.48	7.0	Type IV	29.1	51.4	28.6	30.7
05149	86.11	9.8	No turn	–	–	–	–
05608	85.87	6.5	Type IV	24.5	38.8	29.8	30.8
10003	85.66	9.8	No turn	–	–	–	–
16216	85.66	9.8	No turn	–	–	–	–
27206	85.66	9.7	No turn	–	–	–	–
46303	85.66	9.8	No turn	–	–	–	–
70764	84.31	6.6	Type IV	24.3	37.3	28.5	42.3

\*Reported in the table are: the random conformation number, its energy, the  $C_i^\alpha-C_{i+3}^\alpha$  distance, the type of turn, and the difference between each dihedral angle with the ones of a canonical type VIII (for clarity this latter is only shown in the case of turn conformations).

overall conformation and it is correlated with the  $C_i^\alpha-C_{i+3}^\alpha$  distance:  $\psi$  of Asp-2 in the  $\beta$ -region gives the extended conformation, whereas in the  $\alpha$ -region it gives the turn. The trajectories at other temperatures sample a similar conformational space but with a different kinetics of transitions.

### Comparison of the simulation at 300 K with NMR data

In Table 1, the  $^3J_{NH-H\alpha}$  coupling constants and NOE distances back-calculated from the MD trajectory are compared with the experimental data: all values agree with the experimental ones within the reported standard deviations. This is not the case if only portions of the trajectory corresponding to well-defined extended or  $\beta$ -turn conformations are considered, indicating that a mixture of conformations must exist in solution. For the J-couplings, the value of Asp-2 can be interpreted as an average between extended (major species) and  $\beta$ -turn conformations, while the 7.18-Hz value of the Asn-3 coupling can only be explained by the presence of poly-proline II conformations. The only discrepancy between experimental data and simulation is found for the Asp-2 HN–Asn-3 HN NOE: an average distance of 0.34 nm is calculated from the MD trajectory while this NOE could not be observed experimentally. As already explained above, this NOE should have been detected, because the maximum distance between those protons cannot exceed 0.5 nm. Its absence can be attributed to dynamical effects coming from

the modulation of the  $\psi$ -angle of Asp-2 due to the conformational averaging between extended and turn conformations in solution. In our simulation, we retrieve  $\sim 6\%$  of turn conformations at 300 K.

Finally, we also compared the experimental H $\alpha$  chemical shifts with the values from our MD trajectory (see Table 1) back-calculated using the SHIFTCALC software (100). A reasonably good agreement (within mean  $\pm 1$  SD) is obtained, indicating again that our MD trajectory is consistent with the experimental NMR data (a plot of the distribution of back-calculated chemical shifts is available as Supplementary Material).

### Free energy landscape of GDNP conformations

The free energy landscape of GDNP at 300 K along the two main reaction coordinates ( $\psi_{Asp2}$  and  $\phi_{Asn3}$ ) is presented in Fig. 3, as well as the respective projections along  $\psi_{Asp2}$  and  $\phi_{Asn3}$  for all temperatures. The free energy profile along a reaction coordinate  $\xi$  was evaluated from the probability  $p_\xi$  of finding one particular value of  $\xi$  (using a 5° bin width) with the following formula:

$$\Delta G(\xi) = -RT \log(p_\xi/p_{\xi_{min}}), \quad (1)$$

where  $R$  is the Boltzmann constant,  $T$  the absolute temperature, and  $\xi_{min}$  the conformation of lowest free energy (highest probability).

We find two main attractor basins in the free energy landscape, the deepest one corresponding to extended conformations around  $\psi_{Asp2} = 135^\circ$  and  $\phi_{Asn3} = -130^\circ$ , and another fairly deep one corresponding to turn conformations around  $\psi_{Asp2} = -55^\circ$  and  $\phi_{Asn3} = -125^\circ$ . Interestingly, the two wells identified from the conformational space search (see ‘‘Conformational space exploration’’ section) fit within these two basins, as shown by the red crosses. However, they do not lie exactly at the free energy minimum because their evaluation did not take into account any entropic contribution. This can also be attributed to the fact that the force fields used are different. In each basin, there are two local minima for  $\phi_{Asn3}$ . The first one represents  $\phi$ -values around  $-120^\circ$  ( $\beta$ -conformations), the second one corresponds to values around  $-75^\circ$  (polyproline II conformations). One can notice, too, that there are two other shallow basins for positive values of  $\phi$  around  $+50^\circ$  (left-handed  $\alpha$ -helix conformations), which are, however, significantly less populated. Lastly, conformations with  $\phi$ -values between 100 and  $150^\circ$  are rarely visited indicating a high free energy barrier.

Let us focus now on the projection along  $\psi_{Asp2}$ , the most important degree of freedom of the peptide. On going from extended to  $\beta$ -turn conformations there are two pathways, with two associated transition state energy barriers. The first one ( $\Delta G_1^{++}$ ) corresponds to a value of  $\sim 13$  kJ mol<sup>-1</sup> at  $\psi \sim -120^\circ$  (see Fig. 4 and Table 3) whereas the second ( $\Delta G_2^{++}$ ) is a bit higher with a value of  $\sim 15$  kJ mol<sup>-1</sup> at  $\psi \sim 0^\circ$ . The extended conformations are more populated than the folded

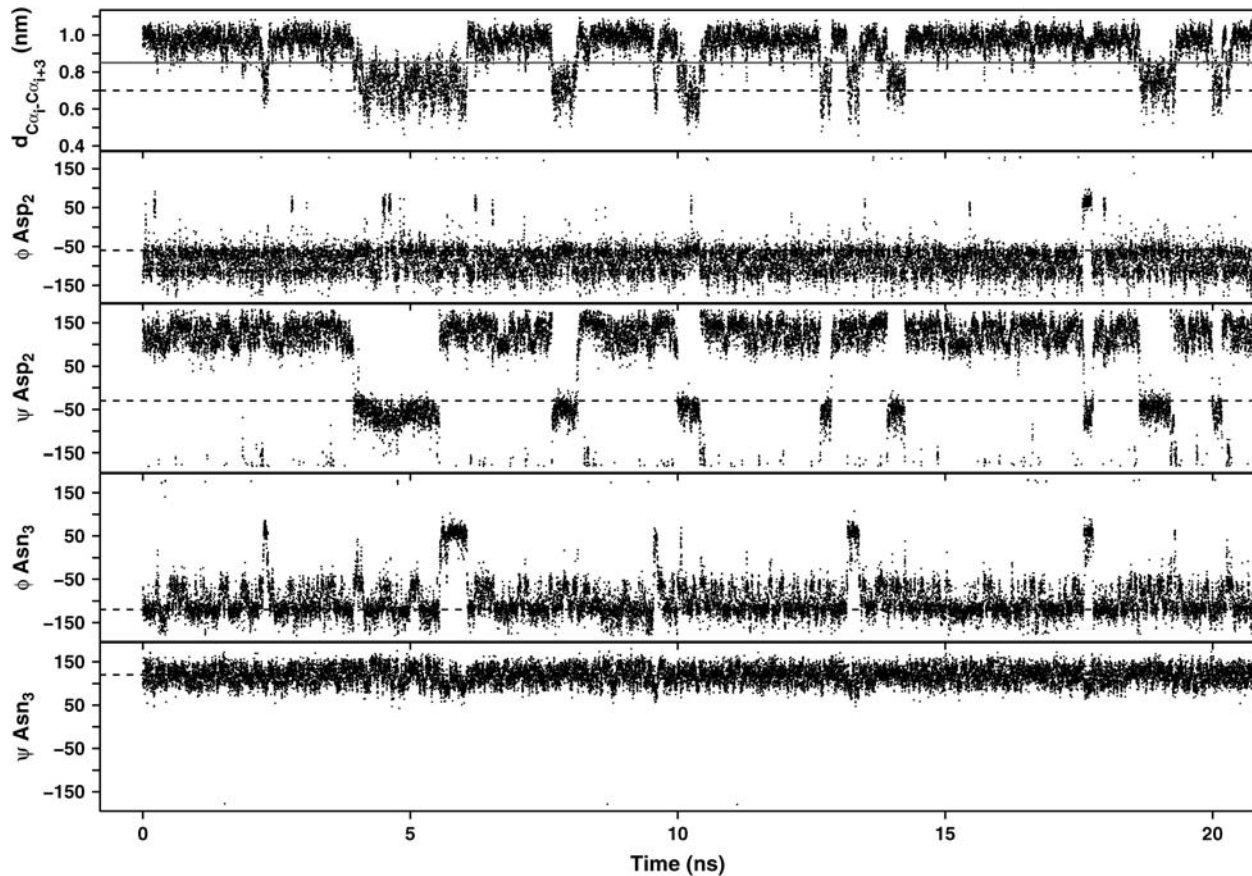


FIGURE 2 Time evolution of  $\phi / \psi$  of residues Asp-2 and Asn-3 and the distance between  $C^{\alpha}_i$  and  $C^{\alpha}_{i+3}$  for the trajectory in water at 300 K (only the first 20 ns are represented for clarity). The horizontal dashed lines in each plot represent the distance below which a turn is defined (0.7 nm) and the canonical values of  $\phi / \psi$  of type VIII  $\beta$ -turn. The solid line in the top panel shows the optimal distance cutoff that separates two groups of conformation.

ones with a free energy difference of  $\sim 4.2 \text{ kJ mol}^{-1}$  at 300 K. Because of this small difference as well as the reasonably low value for  $\Delta G_1^{++}$  and  $\Delta G_2^{++}$  (the transition states free energies) the peptide does go from one state to the other at room temperature. Interestingly, a principal component analysis of the trajectories emphasizes this aspect (see Supplementary Material). The two first principal components (which represent  $\sim 62\%$  of the whole motion) describe the two pathways of type VIII formation: the first one passes via  $\Delta G_1^{++}$  and accounts for  $\sim 36\%$  of the whole peptide motion, whereas the second one passes via  $\Delta G_2^{++}$  and accounts for 26% of the motion. This difference can be accounted for by the fact that  $\Delta G_1^{++}$  is  $2.4 \text{ kJ mol}^{-1}$  lower than  $\Delta G_2^{++}$  at 300 K. As the temperature increases, the first pathway (via  $\Delta G_1^{++}$ ), becomes more frequently used by the peptide because the free energy difference between  $\Delta G_1^{++}$  and  $\Delta G_2^{++}$  increases; as can be seen from the projection along  $\psi_{asp2}$   $\Delta G_1^{++}$  decreases with increasing temperature whereas  $\Delta G_2^{++}$  increases. Even, if it is only a trend, this result is somewhat of a surprise because we would expect a common behavior for both transition states. It means that the conformations and/or the water organization encountered in

the first pathway are favored by a temperature increase whereas those in the second pathway are disfavored.

### Thermodynamic of type VIII folding

The free energy of type VIII folding has been calculated by the Gibbs relationship:

$$\Delta G_{\text{nontypeVIII} \rightarrow \text{typeVIII}} = -RT \log(p_{\text{typeVIII}}/p_{\text{nontypeVIII}}). \quad (2)$$

The convergence of  $\Delta G$  at each temperature is presented in Fig. 5. The first obvious remark is that  $\Delta G$  convergence is very slow: at 340 and 360 K, the final trend occurs after 100 ns whereas at 280 K no clear convergence is observed. Convergence in free energy calculations is a severe problem and is often the limiting step as remarked several times (101,102). This is the case here for the small peptide GDNP for which a few hundred nanoseconds are required to reach convergence. This might be due partly to the small fraction of ideal type VIII conformations within the trajectory that represents 1.77, 1.82, 1.90, 1.75, and 1.83% of the ensemble at 280, 300, 320, 340, and 360 K, respectively. An ‘‘ideal’’  $\beta$ -turn is characterized by a  $C^{\alpha}_i - C^{\alpha}_{i+3}$  distance below 7 Å.

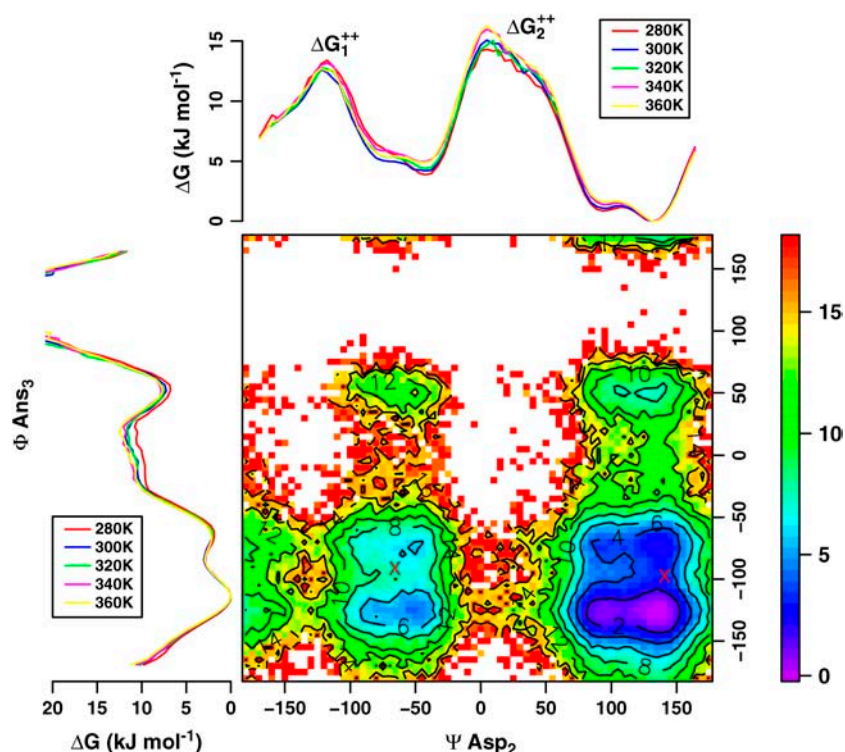


FIGURE 3 Free energy landscape (potential of mean force) of GDNP conformations at 300 K along  $\psi_{\text{Asp}2}$  and  $\phi_{\text{Asn}3}$ . The color scale for the free energy is indicated on the right in  $\text{kJ mol}^{-1}$ . The plots on the left and on the top correspond to the free energy projection at all temperatures on  $\phi_{\text{Asn}3}$  and  $\psi_{\text{Asp}2}$ , respectively. To normalize the values, the lowest one has been fixed arbitrarily to 0. The two red crosses represent the minima we found in the conformational space exploration.

The total fraction of turn conformations whatever the type ( $C_i^\alpha - C_{i+3}^\alpha$  distance below 0.7 nm) is 5.26, 6.05, 6.47, 6.25, and 7.00% at 280, 300, 320, 340, and 360 K, respectively.

The dependence of the free energy of type VIII formation upon temperature is plotted in Fig. 6. It varies linearly with temperature with a correlation coefficient of 0.992 and is always positive meaning that it costs some energy to form type VIII  $\beta$ -turn. The free energy difference remains, however, within a few kT (between 8 and 10.5  $\text{kJ mol}^{-1}$ , which corresponds to 4–5 kT at 300 K) and can be easily overcome by kinetic energy. The linearity of  $\Delta G$  versus temperature enables us to determine the enthalpy and entropy of type VIII  $\beta$ -turn formation (assuming that these two quantities are temperature independent in the range

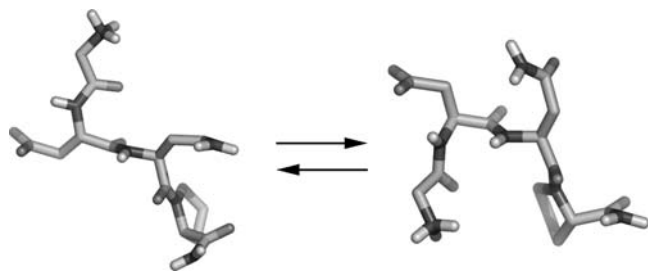


FIGURE 4 Snapshots representing the two free energy minima of the simulation at 300 K. The one on the left corresponds to the extended conformation, and the other to the turn. Only the simulated atoms are represented. These representations were rendered with the PyMOL program (W. L. DeLano, The PyMOL Molecular Graphics System, 2002, <http://www.pymol.org>).

280–360 K):  $\Delta H = -0.061 \text{ kJ mol}^{-1}$  and  $\Delta S = -0.0295 \text{ kJ mol}^{-1} \text{ K}^{-1}$ . At any temperature,  $\Delta H$  is very small whereas  $T\Delta S$  is by far dominant (e.g., 8.84  $\text{kJ mol}^{-1}$  at 300 K). This shows that the process is mainly driven by the entropic contributions. Accordingly, turn formation becomes more and more favorable when the temperature decreases. The small value of  $\Delta H$  is in agreement with the results of the conformational space exploration; it contains, however, in addition the peptide/solvent interaction. These results are in line with another study on blocked dipeptides (48) showing that the turn was intrinsically unstable in absence of stabilizing interactions. Our results indicate that type VIII is not stabilized by any backbone hydrogen bond, and that only side-chain interactions can contribute to the stabilization of the turn: the side chains of Asp-2 and Asn-3 are indeed found to make transient hydrogen bonds with the backbone (e.g., 10% of the time at 280 K). Their occurrence is, however, uncorrelated with the backbone conformation and therefore they cannot be considered as a real type VIII  $\beta$ -turn stabilizing interaction playing a role in the thermodynamic equilibrium.

### Kinetics of type VIII folding

Before addressing the kinetics of type VIII formation we want to emphasize one important point: until now, we took the very strict classical geometrical definition ( $C_i^\alpha - C_{i+3}^\alpha$  distance lower than 0.7 nm and a threshold of  $30^\circ$  on the dihedral angles) for extracting type VIII conformations from

**TABLE 3** Free energy of type VIII  $\beta$ -turn formation and the two transition states calculated along  $\psi_{\text{Asn3}}$ 

Temperature (K)	$\Delta G_{\text{VIII}}^*$ (kJ mol <sup>-1</sup> )	$\Delta G_1^{+\ddagger}$ (kJ mol <sup>-1</sup> )	$\Delta G_2^{+\ddagger}$ (kJ mol <sup>-1</sup> )	$\Delta\Delta G_{1-2}^{\S}$ (kJ mol <sup>-1</sup> )
280	3.9	13.4	14.3	0.9
300	4.2	12.7	15.1	2.4
320	4.4	12.8	15.1	2.3
340	5.0	13.0	16.0	3.0
360	4.9	12.7	16.3	3.6

All the values are calculated compared to the lowest free energy point in the profile (arbitrarily fixed to 0) that occurs at  $\psi \sim 120^\circ$  and corresponds to extended conformations.

\*Free energy of type VIII like conformations (at  $\psi_{\text{Asn3}} \sim -50^\circ$ ).

<sup>†</sup>Free energy of the first transition state (at  $\psi_{\text{Asn3}} \sim -120^\circ$ ).

<sup>‡</sup>Free energy of the second transition state (at  $\psi_{\text{Asn3}} \sim 0^\circ$ ).

<sup>§</sup>Free energy difference between the two transition states ( $\Delta G_1^{+\ddagger}$  and  $\Delta G_2^{+\ddagger}$ ).

our trajectories. This led to very small populations, in the range of 1.8–1.9% for type VIII, and of 5–7% for any type of turn (see above and Fig. 2). Clearly, these criteria are too restrictive and affect the convergence of  $\Delta G$ . By looking at this  $\text{C}\alpha$ – $\text{C}\alpha$  distance in Fig. 2, it is evident that it behaves with a two-states mode; this is further confirmed by the corresponding bimodal distribution (see Fig. 7). One good way to separate these two groups is to set a cutoff of 0.85 nm (see the *solid line* on the *upper plot* of Fig. 2); using this criterion, we reached populations of  $\sim 20\%$  of folded conformations (below 0.85 nm). Of course, these 20% are not all ideal type VIII, but represent globally more compact, turn-like conformers. With this definition, the convergence of  $\Delta G$  of folding is also better and faster (data not shown). To calculate the kinetic rate of passing from extended to type VIII like conformations (thus above and below this 0.85-nm threshold), we evaluated the time spent in each state (before going to the other state). With this simple cutoff approach, we got many meaningless, short periods resulting in unrealistic mean times of type VIII formation. These very short

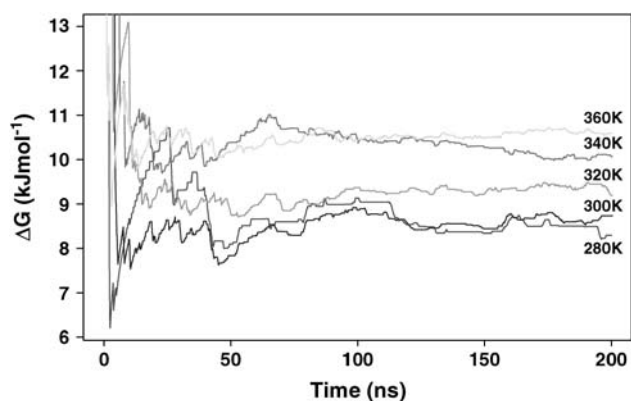


FIGURE 5 Convergence of type VIII  $\beta$ -turn free energy of folding at different temperatures.

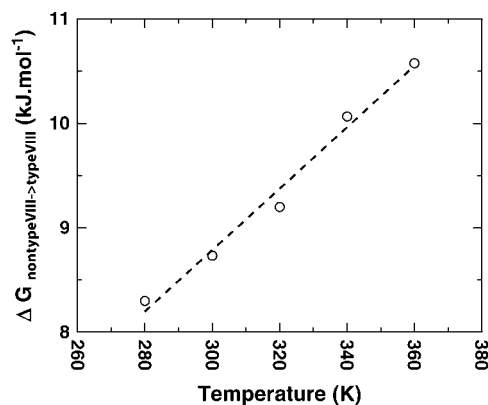


FIGURE 6 Dependence of the free energy of type VIII  $\beta$ -turn folding upon temperature.

times represent fluctuations around the transition state. To get rid of these fluctuations, we considered that a transition from extended (nonturn) to turn had occurred only once the  $\text{C}\alpha$ – $\text{C}\alpha$  distance had passed below 0.7 nm, and from turn to extended once the distance had passed above 0.95 nm.

In Fig. 8 the distributions of folding times at different temperatures as well as the corresponding Arrhenius plot are displayed. These distributions are exponential, and fit rather well to theoretical curves. The fit gets better at higher temperature (the correlation coefficients are 0.866, 0.946, 0.958, 0.968, and 0.988 at 280, 300, 320, 340, and 360 K, respectively), which is easily explained by the fact that there are more transitions in the latter cases. The mean time of folding  $\tau$  can be extracted as the mean of the distribution and corresponds in principle to the decay of the exponential ( $\exp(-t/\tau)$ ) (if the distribution is perfectly exponential). We find a value of  $\sim 1.4$  ns at 300 K, which is consistent with what we observe in Fig. 2. This nanosecond timescale at room temperature is similar to that found by Tobias et al. for type I and II on the YPGDV peptide (47), as well as by

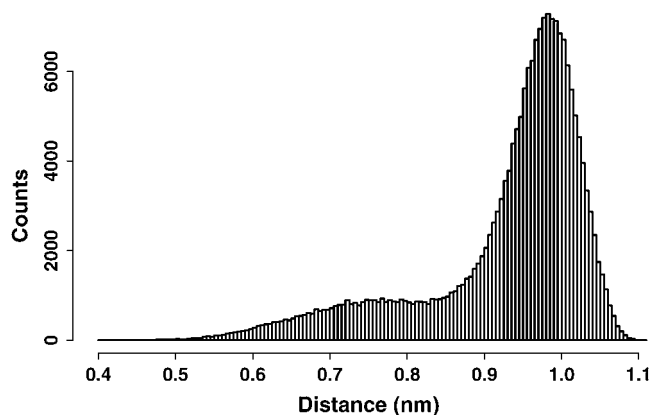


FIGURE 7 Distribution of the  $\text{C}_i^\alpha$  and  $\text{C}_{i+3}^\alpha$  distances from the 300 K MD simulation.

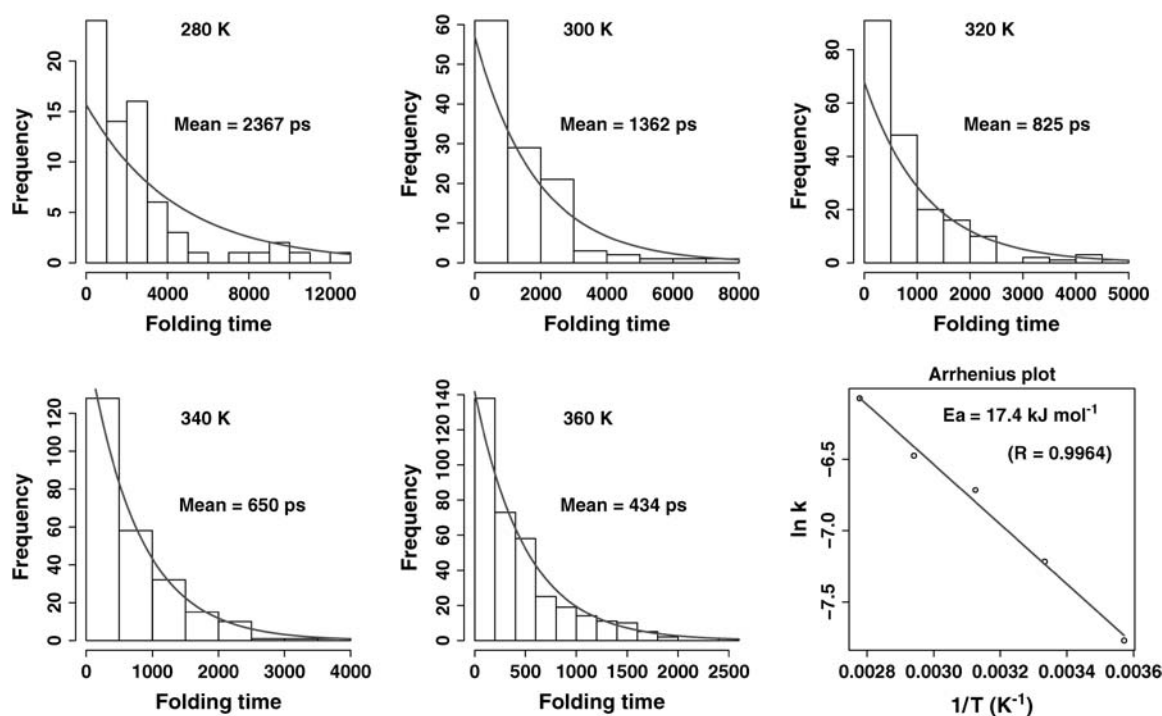


FIGURE 8 Folding kinetics of type VIII  $\beta$ -turn. The first five plots represent the distribution of the folding times at each temperature; within each of these plots, the mean time of folding is indicated (as  $\tau$  in ps); the gray lines correspond to a fit of the distribution to an exponential curve. The last graph is an Arrhenius plot, in which the activation energy is indicated (calculated as  $-\text{slope} \times R$ );  $k$  stands for the rate constant.

Mohanty et al. for type VI on the SYPYD peptide (45). This is also consistent with the work of Hummer et al. (103) on helix nucleation kinetics (i.e., formation of the first  $\alpha$ -helical turn) who found values between 0.1 and 1 ns on some Ala/Gly containing peptides. The last plot of the figure clearly shows that “type VIII like”  $\beta$ -turn formation follows an Arrhenius behavior (with an excellent correlation coefficient of 0.996); the activation energy extracted from the slope gives a value of  $17.4 \text{ kJ mol}^{-1}$  that reflects again the relative ease of type VIII formation. This value is in the same range as the free energy barrier  $\Delta G^{++}$  previously calculated (see Table 3).

## DISCUSSION

We have studied the dynamics of type VIII  $\beta$ -turn formation and showed that for the GDNP sequence, the turn is not the preferred conformation but a possible conformer within the whole population. Moreover, we found that the transition from an extended toward a turn conformation, presents a low free energy barrier that can be easily overcome at room temperature on a nanosecond timescale. Our data agree with the study of Tobias et al. who showed for Ac-Ala-Ala-NHMe and Ac-Ala-Pro-NHMe peptides that reverse turn conformations are intrinsically unstable in water (48). By decomposing the free energy difference, they found that the great stability of the extended conformation comes mainly from a higher peptide-water entropy. We find here the same results

namely that entropy opposes the formation of type VIII  $\beta$ -turn in the GDNP sequence. This effect is somehow general and comes from the fact that turns are more compact than their extended counterpart. Indeed, solvation usually opposes turn formation, because in the turn conformation less polar surface is solvent exposed (41). Our study and that of Tobias et al. (48) is different from many others where the authors found some exceptionally stable turns (41,43,45,46,51,56) because of some strong stabilizing interactions through the side chains. As recently suggested, turn stability strongly depends on side-chain interactions (and is therefore sequence dependent) but might not be the driving force for  $\beta$ -turn formation (42); water is thought to play a very important role in this process (44). The concept of local propensity has been used in a computational study, to explain the high ability of the peptides SYPYD and SYPGD to form a type VI  $\beta$ -turn (with a *cis*-Pro) (45,104). Local propensity originally refers to the high preference of some residues to populate specific zones of the torsional map (i.e., specific values of  $\phi/\psi$ ), such as the  $\phi$  of Pro. However, local propensity can be affected by other factors such as solvation. This is definitely the case in our simulations, as solvation opposes turn formation despite the fact that the turn propensity of Proline is fairly large (because Pro forces the preceding residue in the  $\beta$ -region (98,99)). In fact, the sequence does not particularly stabilize the turn (the potential energy of the turn conformation is almost equal to that of the extended), but drives the peptide toward it because of its large propensity. We see that propensities are good

predictors of  $\beta$ -turn type formation (or preferences), even if the turn conformation is not by far the most populated conformation as is the case here. Nonetheless, this propensity is always intrinsically present and the balance may easily fall on the side of the turn if the peptide is put in a specific environment that favors it, e.g., in a new solvent (TFE), or by the presence of stabilizing flanking residues, etc. This has important consequences for polypeptides that contain the GDNP sequence, and more generally the XXXP motif. Our results suggest that this motif is a real type VIII former.

Some of the  $\beta$ -turn simulations published so far contained a Pro at the  $i + 3$  position. Van der Spoel et al. performed 1-ns MD simulations on FTGP, YTAP, and YTGP (as well as YTGP within the 15 residues N-terminal part of BPTI) (49). They particularly tried to assess whether various force fields could reproduce available NMR data for these peptides. Worth et al. worked on YTGP using multiple MD trajectories of 0.3 ns each, starting from various conformations (50). The main concern of these two articles was to reproduce NMR data and to look carefully at the interaction between the aromatic ring of Tyr-1 and the amide proton of Gly-3. In none of these works did the authors mention the existence of type VIII conformation, even if it is likely that some were present due to the Pro at the  $i + 3$  position (see subsection "Description of the trajectory at 300 K"). Van der Spoel et al. reported that Thr-2 visited the right-handed  $\alpha$ -helix region of the Ramachandran plot (corresponding to that of type VIII) for three of their four peptides; the fourth (YTAP) sampling only extended conformations because of a steric hindrance. A 30-ns simulation of the same peptide (data not shown) revealed, however, the presence of type VIII turns. Considering the mean time of folding found here, an 1-ns simulation is very unlikely to lead to turn formation when starting from an extended conformation. Worth et al. gave slightly more details, and found also that the extended conformer was the most populated one. One of the clusters they found had the following dihedral angles  $\phi_{\text{Thr}2} = -75^\circ$  and  $\psi_{\text{Thr}2} = -35^\circ$ , which are close to the canonical angles for type VIII  $\beta$ -turn. Two features account for the different conformational preferences (and thus the relative population of these conformations) between their peptide (YTGP) and ours (GDNP): i), the presence of an aromatic residue at the first position can allow aromatic ring/amide backbone proton interaction; ii), the glycine at position  $i + 2$  gives more flexibility and allows the peptide to visit some other conformations (according to Worth et al.,  $\psi_{\text{Gly}3}$  is blocked around  $-175^\circ$  because of the effect of Pro-4, but  $\phi_{\text{Gly}3}$  can visit some conformations in the left-handed  $\alpha$ -helix region around  $75^\circ$ ). Even if the conformational populations are different, we see that a proline at  $i + 3$  position enables these sequences to form type VIII (or type VIII "like")  $\beta$ -turn. This has also been confirmed in recent explicit (21), or implicit (64), solvent simulations of bioactive elastin peptides, where type VIII  $\beta$ -turns were found for sequences sharing the GXXP motif.

These results from literature are in line with ours, and indicate that the XXXP motif has a strong intrinsic potentiality to form a type VIII (or type VIII like)  $\beta$ -turn in a variety of context (sequence, solvent, etc.). This has important consequences on peptide and protein folding for all sequences that contain this motif as recently highlighted (56). The ease of turn formation may play a critical role during the folding process, especially at the early stages during secondary structure formation, and especially in the case of  $\beta$ -hairpins. As mentioned above, even if type VIII is not the most populated conformer in the isolated tetrapeptide XXXP, it may become so because of additional interactions from the flanking residues during the hairpin formation. As we saw, the enthalpy of type VIII formation is favorable, and the gain in energy brought by these new interactions may counterbalance the entropic contribution that opposes turn formation in the isolated tetrapeptide. This mechanism of  $\beta$ -hairpin formation where the  $\beta$ -turn forms first has been observed many times experimentally (28–30) as well as in simulations (31–33).  $\beta$ -Turns are now widely accepted to play a key role in protein folding because of their importance in  $\beta$ -hairpin formation (40). Within this context, our results suggest that type VIII may play an important role. Beyond the XXXP motif, type VIII has been shown to form also for completely different sequences, notably SALN and more generally SXXN (56). This work, associated with ours, definitely shows that type VIII can be from now on considered as an important type, even if it is not hydrogen bonded. Its frequency ( $\sim 9\%$ ) in proteins is almost as important as that of type II, and is definitely larger than that of types I' and II' (5,8).

Type VIII has also been shown to be the bioactive conformation within peptides coming from elastin degradation, which makes it very relevant. In 2001, Brassart et al. demonstrated that some elastin derived peptides sharing the motif GXXPG could upregulate matrix metalloproteinase 1; based on CD and  $\beta$ -turn prediction, it has been hypothesized that the bioactive conformation could be a type VIII  $\beta$ -turn in the GXXP tetrapeptide (20). Floquet et al. confirmed this with a detailed study of one of these peptides (VGVAPG), using explicit solvent molecular dynamics and molecular mechanics (21). This hypothesis has also been validated on tropoelastin peptides containing the GXXP motif, by using implicit MD simulations (64): a correlation was found between bioactivity and the ability of a given peptide to exhibit a type VIII conformation. Another example of type VIII  $\beta$ -turn bioactivity is the case of compstatin: this 13-residue cyclic peptide is a potential therapeutic agent (22,63). It contains a type I  $\beta$ -turn at QDWG that has been shown to switch to type VIII during MD simulations (63). This was proposed to be essential for compstatin bioactivity (22,63). These few examples demonstrate that type VIII can be an important structural motif, involved in many biological activities. Prediction and design of bioactive peptides using computational techniques has become common these last years. For example, Oomen et al. recently predicted with

success the immunogenicity of peptide-vaccine candidates using MD (105). In this context, our work will help the design of specific sequences that should form type VIII  $\beta$ -turns by suggesting to use the motif XXXP, to ensure that the only possible type of  $\beta$ -turn formed is type VIII, in equilibrium with extended conformations. Note that the equilibrium between folded (different types of  $\beta$ -turns) and extended (polyproline II,  $\beta$ -strands) conformations also has implication for the mechanistic properties of proteins; such an equilibrium has recently been proposed as essential for the molecular elasticity of elastomeric proteins (61).

Finally, our work has shed some light on the possible CD spectrum signature of type VIII  $\beta$ -turn. The most common types I and II have been well characterized by CD, using among other cyclic peptides to decrease the peptide flexibility and thus favor turn conformations (90,106). Even though these peptides were constrained by cyclization, it was almost impossible to get a pure set of type I (or II) conformations in solution; a mixture is always present. Hence, the pure CD spectra have been established using deconvolution techniques (106,107). One has, however, to be careful in deriving conformational preferences of  $\beta$ -peptides from a CD spectrum: Glättli et al. recently emphasized that it was possible to reproduce CD spectra from various ensembles of conformations (108). In this context, we have to be careful in interpreting our CD spectra. One aspect bringing ambiguity comes from the fact that type VIII is a kind of mixture of types I and II. Indeed, the  $\phi/\psi$  of residue  $i + 1$  are the same as type I, whereas the  $\phi/\psi$  of residue  $i + 2$  are close to that of residue  $i + 1$  of type II. However, our simulation data clearly demonstrate that our peptide can only adopt type VIII or extended conformations, because of the Pro at position  $i + 3$ . The basic shape of our CD spectra (one major negative band at 200 nm and a negative shoulder at 220 nm) has already been met in some other works (92,106), but none of the authors assigned the whole (or a component of the) spectrum to type VIII. This shape may thus not be really typical of type VIII, and we cannot talk of a "specific" signature. Nevertheless, we propose that beyond the shape, the temperature and solvent effects could be indicative of the presence of some type VIII  $\beta$ -turn conformations. To increase the population of type VIII and obtain a clearer CD signature, modified amino acids could be introduced at the  $i + 1$  position to force this residue in the  $\alpha$ -region. For example, Aib ( $\alpha$ -aminoisobutyryl) is known to have such an effect (109).

All this discussion around type VIII, and more generally around  $\beta$ -turns definitely shows their importance in peptide and protein chemistry, biophysics, and bioinformatics. Many efforts have been devoted to characterize them experimentally and link the results to simulation data, like in a recent work on type II' (110). Some promising experimental approaches that have been recently used to characterize  $\beta$ -turns are ultraviolet and infrared spectroscopies in the gas phase. Using such techniques, the behavior of residues under isolated conditions (i.e., the gas phase) was shown to be con-

sistent with  $\beta$ -turn residue propensities in proteins (111). All the work in this area has so far been devoted to types I and II, and to a lesser extent to type I' and II' (111–114). One way to improve our knowledge on type VIII would thus be to characterize it by optical spectroscopies (Raman, infrared, Fourier transform infrared, ultraviolet).

## SUPPLEMENTARY MATERIAL

An online supplement to this article can be found by visiting BJ Online at <http://www.biophysj.org>.

We gratefully acknowledge members of the Equipe de Bioinformatique Génomique et Moléculaire for useful discussions, especially S. Hazout, F. Guyon, and C. Etchebest. K. Pakdaman is also acknowledged for fruitful discussion on the kinetic aspect. P.F. dedicates this work to the memory of Prof. S. Hazout.

## REFERENCES

- Venkatachalam, C. M. 1968. Stereochemical criteria for polypeptides and proteins. V. Conformation of a system of three linked peptide units. *Biopolymers*. 6:1425–1436.
- Lewis, P. N., F. A. Momany, and H. A. Scheraga. 1973. Chain reversals in proteins. *Biochim. Biophys. Acta*. 303:211–229.
- Richardson, J. S. 1981. The anatomy and taxonomy of protein structure. *Adv. Protein Chem.* 34:167–339.
- Wilmot, C. M., and J. M. Thornton. 1988. Analysis and prediction of the different types of beta-turn in proteins. *J. Mol. Biol.* 203:221–232.
- Hutchinson, E. G., and J. M. Thornton. 1994. A revised set of potentials for beta-turn formation in proteins. *Protein Sci.* 3:2207–2216.
- Rose, G. D., L. M. Gierasch, and J. A. Smith. 1985. Turns in peptides and proteins. *Adv. Protein Chem.* 37:1–109.
- Lagunez-Otero, J., A. Diaz-Villasenor, and V. Renugopalakrishnan. 2002. Specialized biology from tandem beta-turns. *Arch. Med. Res.* 33:245–249.
- Fuchs, P. F. J., and A. J. P. Alix. 2005. High accuracy prediction of beta-turns and their types using propensities and multiple alignments. *Proteins*. 59:828–839.
- Brooks, C. L., M. Karplus, and B. M. Pettitt. 1988. Protein. A theoretical perspective of dynamics, structure and thermodynamics. Wiley-Interscience, New York.
- Karplus, M., and G. A. Petsko. 1990. Molecular dynamics simulations in biology. *Nature*. 347:631–639.
- Karplus, M., and J. A. McCammon. 2002. Molecular dynamics simulations of biomolecules. *Nat. Struct. Biol.* 9:646–652.
- Gerstein, M., and N. Echols. 2004. Exploring the range of protein flexibility, from a structural proteomics perspective. *Curr. Opin. Chem. Biol.* 8:14–19.
- Teague, S. J. 2003. Implications of protein flexibility for drug discovery. *Nat. Rev. Drug Discov.* 2:527–541.
- Erickson, J. A., M. Jalaie, D. H. Robertson, R. A. Lewis, and M. Vieth. 2004. Lessons in molecular recognition: the effects of ligand and protein flexibility on molecular docking accuracy. *J. Med. Chem.* 47:45–55.
- Halperin, I., B. Ma, H. Wolfson, and R. Nussinov. 2002. Principles of docking: an overview of search algorithms and a guide to scoring functions. *Proteins*. 47:409–443.
- van Dijk, A. D., R. Boelens, and A. M. Bonvin. 2005. Data-driven docking for the study of biomolecular complexes. *FEBS J.* 272: 293–312.

17. DeBelle, L., and A. M. Tamburro. 1999. Elastin: molecular description and function. *Int. J. Biochem. Cell Biol.* 31:261–272.
18. Tamburro, A. M. 1990. Order-disorder in the structure of elastin: a synthetic approach. In *Elastin: Chemical and Biological Aspects*. A. M. Tamburro and J. Davidson, editors. Congedo, Galatina, Italy. 125–145.
19. Leij, F., A. M. Tamburro, V. Villani, P. Grimaldi, and V. Guantieri. 1992. Molecular dynamics study of the conformational behavior of a representative elastin building block: Boc-Gly-Val-Gly-Gly-Leu-OMe. *Biopolymers*. 32:161–172.
20. Brassart, B., P. F. J. Fuchs, E. Huet, A. J. P. Alix, J. Wallach, A. M. Tamburro, F. Delacoux, B. Haye, H. Emonard, W. Hornebeck, and L. DeBelle. 2001. Conformational dependence of collagenase (matrix metalloproteinase-1) up-regulation by elastin peptides in cultured fibroblasts. *J. Biol. Chem.* 276:5222–5227.
21. Floquet, N., S. Héry-Huynh, M. Dauchez, P. Derreumaux, A. M. Tamburro, and A. J. P. Alix. 2004. Structural characterization of VGVAPG, an elastin-derived peptide. *Biopolymers*. 76:266–280.
22. Morikis, D., M. Roy, A. Sahu, A. Troganis, P. A. Jennings, G. C. Tsokos, and J. D. Lambris. 2002. The structural basis of compstatin activity examined by structure-function-based design of peptide analogs and NMR. *J. Biol. Chem.* 277:14942–14953.
23. Muller, G., G. Hessler, and H. Y. Decornez. 2000. Are beta-turn mimetics mimics of beta-turns? *Angew. Chem. Int. Ed. Engl.* 39: 894–896.
24. Kee, K. S., and S. D. Jois. 2003. Design of beta-turn based therapeutic agents. *Curr. Pharm. Des.* 9:1209–1224.
25. Blanco, F., M. Ramirez-Alvarado, and L. Serrano. 1998. Formation and stability of beta-hairpin structures in polypeptides. *Curr. Opin. Struct. Biol.* 8:107–111.
26. de Alba, E., M. A. Jimenez, and M. Rico. 1997. Turn residue sequence determines beta-hairpin conformation in designed peptides. *J. Am. Chem. Soc.* 119:175–183.
27. de Alba, E., M. Rico, and M. A. Jimenez. 1999. The turn sequence directs beta-strand alignment in designed beta-hairpins. *Protein Sci.* 8:2234–2244.
28. Munoz, V., P. A. Thompson, J. Hofrichter, and W. A. Eaton. 1997. Folding dynamics and mechanism of beta-hairpin formation. *Nature*. 390:196–199.
29. Ramirez-Alvarado, M., F. J. Blanco, H. Niemann, and L. Serrano. 1997. Role of beta-turn residues in beta-hairpin formation and stability in designed peptides. *J. Mol. Biol.* 273:898–912.
30. Santiveri, C. M., J. Santoro, M. Rico, and M. A. Jimenez. 2002. Thermodynamic analysis of beta-hairpin-forming peptides from the thermal dependence of (1)H NMR chemical shifts. *J. Am. Chem. Soc.* 124:14903–14909.
31. Bonvin, A. M., and W. F. van Gunsteren. 2000. Beta-hairpin stability and folding: molecular dynamics studies of the first beta-hairpin of tendamistat. *J. Mol. Biol.* 296:255–268.
32. Cavalli, A., P. Ferrara, and A. Caffisch. 2002. Weak temperature dependence of the free energy surface and folding pathways of structured peptides. *Proteins*. 47:305–314.
33. Ferrara, P., A. Joannis, and A. Caffisch. 2000. Thermodynamics and kinetics of folding of two model peptides investigated by molecular dynamics simulations. *J. Phys. Chem. B*. 104:5000–5010.
34. Dinner, A. R., T. Lazaridis, and M. Karplus. 1999. Understanding beta-hairpin formation. *Proc. Natl. Acad. Sci. USA*. 96:9068–9073.
35. Pande, V. S., and D. S. Rokhsar. 1999. Molecular dynamics simulations of unfolding and refolding of a beta-hairpin fragment of protein G. *Proc. Natl. Acad. Sci. USA*. 96:9062–9067.
36. Wei, G., N. Mousseau, and P. Derreumaux. 2004. Complex folding pathways in a simple beta-hairpin. *Proteins*. 56:464–474.
37. Gu, H., D. Kim, and D. Baker. 1997. Contrasting roles for symmetrically disposed beta-turns in the folding of a small protein. *J. Mol. Biol.* 274:588–596.
38. Kim, J., S. R. Brych, J. Lee, T. M. Logan, and M. Blaber. 2003. Identification of a key structural element for protein folding within beta-hairpin turns. *J. Mol. Biol.* 328:951–961.
39. Platt, G. W., S. A. Simpson, R. Layfield, and M. S. Searle. 2003. Stability and folding kinetics of a ubiquitin mutant with a strong propensity for nonnative beta-hairpin conformation in the unfolded state. *Biochemistry*. 42:13762–13771.
40. Searle, M. S., and B. Ciani. 2004. Design of beta-sheet systems for understanding the thermodynamics and kinetics of protein folding. *Curr. Opin. Struct. Biol.* 14:458–464.
41. Bashford, D., D. A. Case, C. Choi, and G. P. Gippert. 1997. A computational study of the role of solvation effects in reverse turn formation in the tetrapeptides APGD and APGN. *J. Am. Chem. Soc.* 119:4964–4971.
42. Borics, A., R. F. Murphy, and S. Lovas. 2004. Molecular dynamics simulations of beta-turn forming tetra- and hexapeptides. *J. Biomol. Struct. Dyn.* 21:761–770.
43. Demchuk, E., D. Bashford, and D. A. Case. 1997. Dynamics of a type VI reverse turn in a linear peptide in aqueous solution. *Fold. Des.* 2:35–46.
44. Karvounis, G., D. Nerukh, and R. C. Glen. 2004. Water network dynamics at the critical moment of a peptide's beta-turn formation: a molecular dynamics study. *J. Chem. Phys.* 121:4925–4935.
45. Mohanty, D., R. Elber, D. Thirumalai, D. Beglov, and B. Roux. 1997. Kinetics of peptide folding: computer simulations of SYPFDV and peptide variants in water. *J. Mol. Biol.* 272:423–442.
46. Scully, J., and J. Hermans. 1994. Backbone flexibility and stability of reverse turn conformation in a model system. *J. Mol. Biol.* 235: 682–694.
47. Tobias, D. J., J. E. Mertz, and C. L. Brooks III. 1991. Nanosecond time scale folding dynamics of a pentapeptide in water. *Biochemistry*. 30:6054–6058.
48. Tobias, D. J., S. F. Sneddon, and C. L. Brooks III. 1990. Reverse turns in blocked dipeptides are intrinsically unstable in water. *J. Mol. Biol.* 216:783–796.
49. van der Spoel, D., A. R. van Buuren, D. P. Tieleman, and H. J. Berendsen. 1996. Molecular dynamics simulations of peptides from BPTI: a closer look at amide-aromatic interactions. *J. Biomol. NMR*. 8:229–238.
50. Worth, G. A., F. Nardi, and R. C. Wade. 1998. Use of multiple molecular dynamics trajectories to study biomolecules in solution: the YTGP peptide. *J. Phys. Chem. B*. 102:6260–6272.
51. Wu, X., and S. Wang. 2000. Folding studies of a linear pentamer peptide adopting a reverse turn conformation in aqueous solution through molecular dynamics simulation. *J. Phys. Chem. B*. 104:8023–8034.
52. Demchuk, E., D. Bashford, G. P. Gippert, and D. A. Case. 1997. Thermodynamics of a reverse turn motif. Solvent effects and side-chain packing. *J. Mol. Biol.* 270:305–317.
53. Gnanakaran, S., H. Nymeyer, J. Portman, K. Y. Sanbonmatsu, and A. E. Garcia. 2003. Peptide folding simulations. *Curr. Opin. Struct. Biol.* 13:168–174.
54. Lazaridis, T., D. J. Tobias, C. L. Brooks 3rd, and M. E. Paulaitis. 1991. Reaction paths and free energy profiles for conformational transitions: an internal coordinate approach. *J. Chem. Phys.* 95:7612–7625.
55. Nakajima, N., J. Higo, A. Kidera, and H. Nakamura. 2000. Free energy landscapes of peptides by enhanced conformational sampling. *J. Mol. Biol.* 296:197–216.
56. Santa, H., M. Ylisirnio, T. Hassinen, R. Laatikainen, and M. Perakyla. 2002. Stability and amino acid preferences of type VIII reverse turn: the most common turn in peptides? *Protein Eng.* 15: 651–657.

57. Yan, Y., B. W. Erickson, and A. Tropsha. 1995. Free energies for folding and refolding of four types of beta-turns: simulation of the role of D/L chirality. *J. Am. Chem. Soc.* 117:7592–7599.
58. Yan, Y., A. Tropsha, J. Hermans, and B. W. Erickson. 1993. Free energies for refolding of the common beta turn into the inverse-common beta turn: simulation of the role of D/L chirality. *Proc. Natl. Acad. Sci. USA.* 90:7898–7902.
59. Yang, A. S., B. Hitz, and B. Honig. 1996. Free energy determinants of secondary structure formation. III. Beta-turns and their role in protein folding. *J. Mol. Biol.* 259:873–882.
60. Hansmann, U. H. E., and J. N. Onuchic. 2001. Thermodynamics and kinetics of folding of a small peptide. *J. Chem. Phys.* 115:1601–1606.
61. Tamburro, A. M., B. Bochicchio, and A. Pepe. 2003. Dissection of human tropoelastin: exon-by-exon chemical synthesis and related conformational studies. *Biochemistry.* 42:13347–13362.
62. Sowdhamini, R., N. Srinivasan, C. Ramakrishnan, and P. Balaram. 1992. Orthogonal beta beta motifs in proteins. *J. Mol. Biol.* 223:845–851.
63. Mallik, B., J. D. Lambris, and D. Morikis. 2003. Conformational interconversion in compstatin probed with molecular dynamics simulations. *Proteins.* 53:130–141.
64. Moroy, G., A. J. P. Alix, and S. Héry-Huynh. 2005. Structural characterization of human elastin derived peptides containing the GXXP sequence. *Biopolymers.* 78:206–220.
65. Santa, H., M. Perakyla, and R. Laatikainen. 1999. Folding of alpha(r)beta and epsilonbeta reverse turns; a nanosecond molecular dynamics simulation of the hexapeptide MSALNT and the octapeptide NMSALNTL in water. *J. Biomol. Struct. Dyn.* 16:1033–1041.
66. Creighton, C. J., C. H. Reynolds, D. H. Lee, G. C. Leo, and A. B. Reitz. 2001. Conformational analysis of the eight-membered ring of the oxidized cysteinyl-cysteine unit implicated in nicotinic acetylcholine receptor ligand recognition. *J. Am. Chem. Soc.* 123:12664–12669.
67. Hudaky, I., Z. Gaspari, O. Carugo, M. Cemazar, S. Pongor, and A. Perczel. 2004. Vicinal disulfide bridge conformers by experimental methods and by ab initio and DFT molecular computations. *Proteins.* 55:152–168.
68. Carugo, O., M. Cemazar, S. Zahariev, I. Hudaky, Z. Gaspari, A. Perczel, and S. Pongor. 2003. Vicinal disulfide turns. *Protein Eng.* 16:637–639.
69. Daura, X., A. Glattli, P. Gee, C. Peter, and W. F. van Gunsteren. 2002. Unfolded state of peptides. *Adv. Protein Chem.* 62:341–360.
70. van Gunsteren, W. F., R. Burgi, C. Peter, and X. Daura. 2001. The key to solving the protein-folding problem lies in an accurate description of the denatured state. *Angew. Chem. Int. Ed. Engl.* 40:351–355.
71. Daggett, V. 2000. Long timescale simulations. *Curr. Opin. Struct. Biol.* 10:160–164.
72. Daura, X., B. Jaun, D. Seebach, W. F. van Gunsteren, and A. E. Mark. 1998. Reversible peptide folding in solution by molecular dynamics simulation. *J. Mol. Biol.* 280:925–932.
73. Daura, X., W. F. van Gunsteren, and A. E. Mark. 1999. Folding-unfolding thermodynamics of a beta-heptapeptide from equilibrium simulations. *Proteins.* 34:269–280.
74. Chipot, C., B. Maigret, and A. Pohorille. 1999. Early events in the folding of an amphipathic peptide: a multianosecond molecular dynamics study. *Proteins.* 36:383–399.
75. Chipot, C., and A. Pohorille. 1998. Folding and translocation of the undecamer of poly-L-leucine across the water-hexane interface. A molecular dynamics study. *J. Am. Chem. Soc.* 120:11912–11924.
76. Duan, Y., and P. A. Kollman. 1998. Pathways to a protein folding intermediate observed in a 1-microsecond simulation in aqueous solution. *Science.* 282:740–744.
77. Shirts, M. R., and V. S. Pande. 2000. Screen savers of the world, unite! *Science.* 290:1903–1904.
78. Fuchs, P. F. J., L. DeBelle, and A. J. P. Alix. 2001. Structural study of some specific elastin hexapeptides activating MMP1. *J. Mol. Struct.* 565–566:335–339.
79. Brooks, B. R., R. E. Bruccoleri, B. D. Olafson, D. J. States, S. Swaminathan, and M. Karplus. 1983. CHARMM: a program for macromolecular energy minimization and dynamics calculations. *J. Comput. Chem.* 4:187–217.
80. MacKerrel, A. D., Jr., D. Bashford, M. Bellott, R. L. Dunbrack, Jr., J. D. Evanseck, M. J. Field, S. Fisher, J. Gao, H. Guo, S. Ha, D. Joseph-MacCarthy, L. Kuchnir, et al. 1998. All-atom empirical potential for molecular modeling and dynamics studies of proteins. *J. Phys. Chem. B.* 102:3586–3616.
81. Berendsen, H. J. C., D. van der Spoel, and R. van Drunen. 1995. GROMACS: a message-passing parallel molecular dynamics implementation. *Comput. Phys. Commun.* 91:43–56.
82. Lindahl, E., B. Hess, and D. van der Spoel. 2001. GROMACS 3.0: a package for molecular simulation and trajectory analysis. *J. Mol. Model. (Online).* 7:306–317.
83. Daura, X., A. E. Mark, and W. F. van Gunsteren. 1998. Parameterization of aliphatic CHn united atoms of GROMOS96 force field. *J. Comput. Chem.* 19:535–547.
84. Berendsen, H. J. C., J. P. M. Postma, W. F. van Gunsteren, and J. Hermans. 1981. Interaction models for water in relation to protein hydration. In *Intermolecular Forces*. B. Pullman, editor. Reidel, Dordrecht, The Netherlands. 331–342.
85. Reference deleted in proof.
86. Berendsen, H. J. C., J. P. M. Postma, A. DiNola, and J. R. Haak. 1984. Molecular dynamics with coupling to an external bath. *J. Chem. Phys.* 81:3684–3690.
87. Hess, B., H. Bekker, H. J. C. Berendsen, and J. G. E. M. Fraaije. 1997. LINCS: a linear constraint solver for molecular simulations. *J. Comput. Chem.* 18:1463–1472.
88. Miyamoto, S., and P. A. Kollman. 1992. SETTLE: an analytical version of the SHAKE and RATTLE algorithms for rigid water models. *J. Comput. Chem.* 13:952–962.
89. Tironi, I. G., R. Sperb, P. E. Smith, and W. F. van Gunsteren. 1995. Generalized reaction field method for molecular dynamics simulations. *J. Chem. Phys.* 102:5451–5459.
90. Woody, R. W. 1995. Circular dichroism. *Methods Enzymol.* 246:34–71.
91. Tamburro, A. M., V. Guantieri, L. Pandolfo, and A. Scopa. 1990. Synthetic fragments and analogues of elastin. II. Conformational studies. *Biopolymers.* 29:855–870.
92. Bienkiewicz, E. A., A. Moon Woody, and R. W. Woody. 2000. Conformation of the RNA polymerase II C-terminal domain: circular dichroism of long and short fragments. *J. Mol. Biol.* 297:119–133.
93. Reiersen, H., and A. R. Rees. 2000. Trifluoroethanol may form a solvent matrix for assisted hydrophobic interactions between peptide side chains. *Protein Eng.* 13:739–743.
94. Tamburro, A. M., V. Guantieri, A. Scopa, and J. M. Drabble. 1991. Polypeptide models of elastin: CD and NMR studies on synthetic poly(X-Gly-Gly). *Chirality.* 3:318–323.
95. Bochicchio, B., and A. M. Tamburro. 2002. Polyproline II structure in proteins: identification by chiroptical spectroscopies, stability, and functions. *Chirality.* 14:782–792.
96. Wüthrich, K. 1986. *NMR of Proteins and Nucleic Acids*. Wiley-Interscience, New-York, Chichester, Brisbane, Toronto, Singapore.
97. Zhang, H., S. Neal, and D. S. Wishart. 2003. RefDB: a database of uniformly referenced protein chemical shifts. *J. Biomol. NMR.* 25: 173–195.
98. MacArthur, M. W., and J. M. Thornton. 1991. Influence of proline residues on protein conformation. *J. Mol. Biol.* 218:397–412.
99. Schimmel, P. R., and P. J. Flory. 1968. Conformational energies and configurational statistics of copolypeptides containing L-proline. *J. Mol. Biol.* 34:105–120.

100. Williamson, M., and M. Refaee. 2004. SHIFTCALC (<http://www.shef.ac.uk/NMR/mainpage.html>).
101. Chipot, C., and D. A. Pearlman. 2002. Free energy calculations. The long and winding gilded road. *Mol Sim.* 28:1–12.
102. van Gunsteren, W. F., X. Daura, and A. E. Mark. 2002. Computation of free energy. *Helv. Chim. Acta.* 85:3113–3129.
103. Hummer, G., A. E. Garcia, and S. Garde. 2001. Helix nucleation kinetics from molecular simulations in explicit solvent. *Proteins.* 42:77–84.
104. Mohanty, D., R. Elber, and D. Thirumalai. 2000. Probing the role of local propensity in peptide turn formation. *Int. J. Quantum Chem.* 80:1125–1128.
105. Oomen, C. J., P. Hoogerhout, A. M. Bonvin, B. Kuipers, H. Brugghe, H. Timmermans, S. R. Haseley, L. van Alphen, and P. Gros. 2003. Immunogenicity of peptide-vaccine candidates predicted by molecular dynamics simulations. *J. Mol. Biol.* 328:1083–1089.
106. Perczel, A., M. Hollosi, B. M. Foxman, and G. D. Fasman. 1991. Conformational analysis of pseudocyclic hexapeptides based on quantitative circular dichroism (CD), NOE, and x-ray data. The pure CD spectra of type I and type II beta-turns. *J. Am. Chem. Soc.* 113:9772–9784.
107. Perczel, A., M. Hollosi, P. Sandor, and G. D. Fasman. 1993. The evaluation of type I and type II beta-turn mixtures. Circular dichroism, NMR and molecular dynamics studies. *Int. J. Pept. Protein Res.* 41:223–236.
108. Glatli, A., X. Daura, D. Seebach, and W. F. van Gunsteren. 2002. Can one derive the conformational preference of a beta-peptide from its CD spectrum? *J. Am. Chem. Soc.* 124:12972–12978.
109. Venkatraman, J., S. C. Shankaramma, and P. Balaram. 2001. Design of folded peptides. *Chem. Rev.* 101:3131–3152.
110. Gibbs, A. C., T. C. Bjorndahl, R. S. Hodges, and D. S. Wishart. 2002. Probing the structural determinants of type II' beta-turn formation in peptides and proteins. *J. Am. Chem. Soc.* 124:1203–1213.
111. Chin, W., J. P. Dognon, F. Piuzzi, B. Tardivel, I. Dimicoli, and M. Mons. 2005. Intrinsic folding of small peptide chains: spectroscopic evidence for the formation of beta-turns in the gas phase. *J. Am. Chem. Soc.* 127:707–712.
112. Cai, S., and B. R. Singh. 1999. Identification of beta-turn and random coil amide III infrared bands for secondary structure estimation of proteins. *Biophys. Chem.* 80:7–20.
113. Hollosi, M., Z. Majer, A. Z. Ronai, A. Magyar, K. Medzihradsky, S. Holly, A. Perczel, and G. D. Fasman. 1994. CD and Fourier transform IR spectroscopic studies of peptides. II. Detection of beta-turns in linear peptides. *Biopolymers.* 34:177–185.
114. Mantsch, H. H., A. Perczel, M. Hollosi, and G. D. Fasman. 1993. Characterization of beta-turns in cyclic hexapeptides in solution by Fourier transform IR spectroscopy. *Biopolymers.* 33:201–207.